

ORBITAL DYNAMICS OF MULTI-PLANET SYSTEMS WITH ECCENTRICITY DIVERSITY

STEPHEN R. KANE¹, SEAN N. RAYMOND^{2,3}

Submitted for publication in the Astrophysical Journal

ABSTRACT

Since exoplanets were detected using the radial velocity method, they have revealed a diverse distribution of orbital configurations. Amongst these are planets in highly eccentric orbits ($e > 0.5$). Most of these systems consist of a single planet but several have been found to also contain a longer period planet in a near-circular orbit. Here we use the latest Keplerian orbital solutions to investigate four known systems which exhibit this extreme eccentricity diversity; HD 37605, HD 74156, HD 163607, and HD 168443. We place limits on the presence of additional planets in these systems based on the radial velocity residuals. We show that the two known planets in each system exchange angular momentum through secular oscillations of their eccentricities. We calculate the amplitude and timescale for these eccentricity oscillations and associated periastron precession. We further demonstrate the effect of mutual orbital inclinations on the amplitude of high-frequency eccentricity oscillations. Finally, we discuss the implications of these oscillations in the context of possible origin scenarios for unequal eccentricities.

Subject headings: planetary systems – techniques: radial velocities – stars: individual (HD 37605, HD 74156, HD 163607, HD 168443)

1. INTRODUCTION

The discovery of exoplanets has yielded many surprises with regards to their properties in comparison with the planets in our Solar System. Amongst these are planets in highly eccentric orbits ($e > 0.5$), such as 16 Cyg B b (Cochran et al. 1997) and HD 80606b (Naef et al. 2001). The number of detected exoplanets is sufficient to note a divergence from circular orbits which occurs beyond a semi-major axis of ~ 0.1 AU (Butler et al. 2006). There is evidence that this correlation is also present in the exoplanetary candidates discovered by the Kepler mission (Kane et al. 2012a), along with evidence that eccentricities tend to decrease with decreasing planetary size. For planets below the size of Neptune, orbits are more likely to be circular since these planets cannot efficiently excite the eccentricities of other planets so collisions are favored over scattering (Goldreich et al. 2004). The more efficient tidal dissipation in this regime also leads to shorter tidal circularization time scales (Goldreich & Soter 1966).

The discovery of planets in highly eccentric orbits, particularly in multi-planet systems, presented a challenge for formation and dynamical models. Significant progress has been made in the meantime towards understanding these interesting systems (e.g., Rasio & Ford (1996); Weidenschilling & Marzari (1996); Lin & Ida (1997)). For multi-planet systems, additional constraints are imposed on eccentricity values due to the requirement that the system remain dynamically sta-

ble. Dynamical interactions of multi-planet systems in the context of eccentricity and formation models have been investigated by numerous authors (Ford & Rasio 2008; Jurić & Tremaine 2008; Malmberg & Davies 2008; Matsumura et al. 2008; Raymond et al. 2008, 2010; Wang & Ford 2011; Timpe et al. 2013). From the known multi-planet systems, there are four in particular which stand out with respect to the diversity of eccentricities present within the system. These are the HD 37605 (Cochran et al. 2011; Wang et al. 2012), HD 74156 (Naef et al. 2004; Meschiari et al. 2011), HD 163607 (Giguere et al. 2012), and HD 168443 (Marcy et al. 1999, 2001; Pilyavsky et al. 2011) systems. Each of these systems contain two giant planets where the inner planet has an eccentricity larger than 0.5 whereas the orbit of the outer planet is much closer to circular. It was shown by Laughlin & Chambers (2001) that dynamical interactions between exoplanets can also result in subsequent radial velocity variations that diverge from Keplerian orbital assumptions. It is therefore interesting to consider the dynamical history and stability of these systems as well as scenarios for their origins.

In this paper we present a detailed study of these four systems with high eccentricity diversity. In Section 2 we summarize the orbital configurations and system parameters for the systems discussed in this study. In Section 3 we utilize the radial velocity solutions for these systems to place quantitative limits on additional planets in each system. Section 4 presents the dynamical analysis of each system including the oscillations of the planet orbital eccentricities and associated periastron precession. In Section 5 we discuss the effects of mutual inclinations on the dynamical stabilities. Section 6 attempts to explore the origins of systems with such eccentricity diversity based on our simulations. We discuss further implications of these analyses in Section 7 and then provide concluding remarks in Section 8.

2. SYSTEM PARAMETERS

skane@sfsu.edu

¹ Department of Physics & Astronomy, San Francisco State University, 1600 Holloway Avenue, San Francisco, CA 94132, USA

² CNRS, UMR 5804, Laboratoire d'Astrophysique de Bordeaux, 2 rue de l'Observatoire, BP 89, F-33271 Floirac Cedex, France

³ Université de Bordeaux, Observatoire Aquitain des Sciences de l'Univers, 2 rue de l'Observatoire, BP 89, F-33271 Floirac Cedex, France

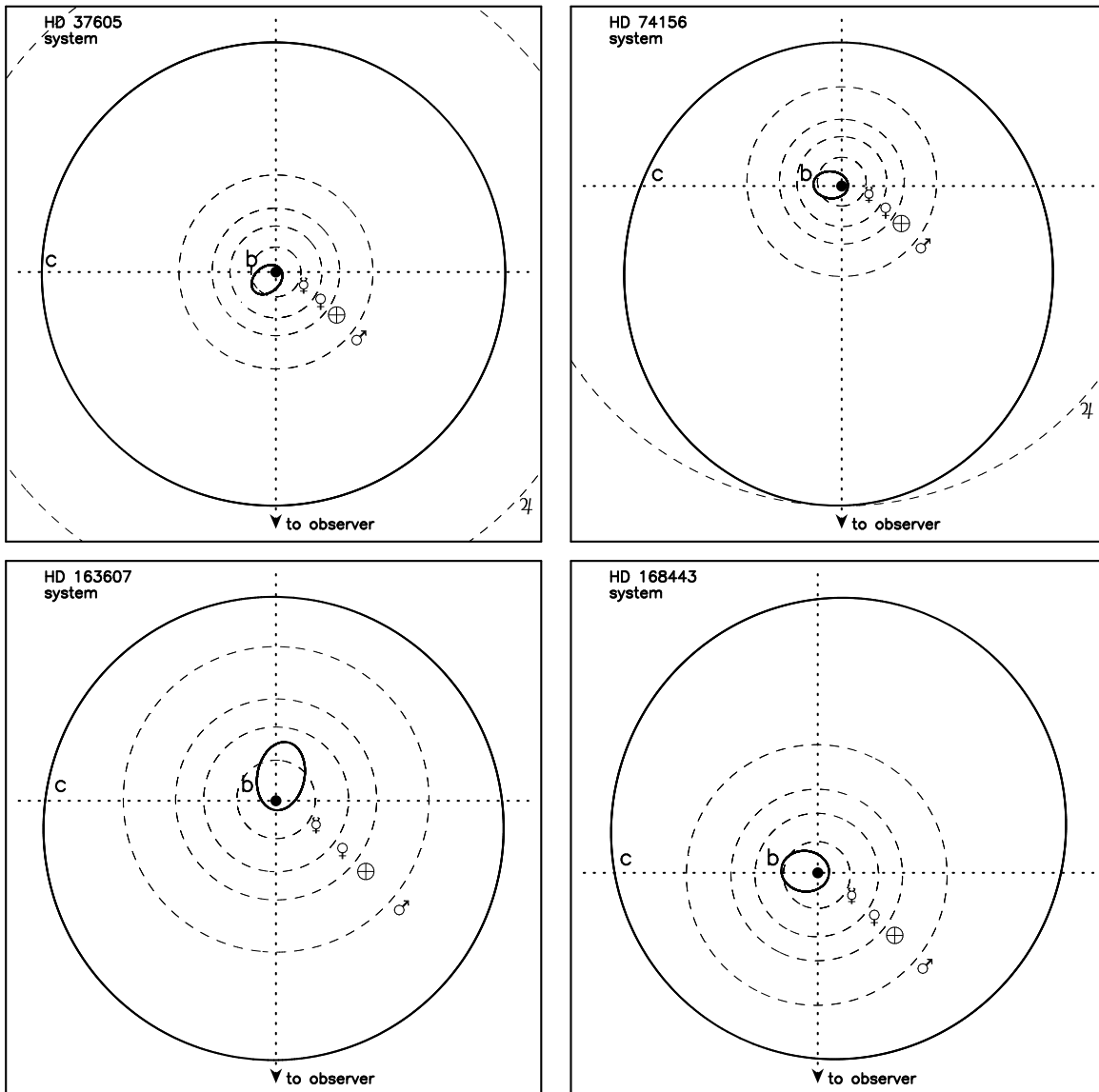


FIG. 1.— A top-down view of each system described in the paper: HD 37605 (top-left), HD 74156 (top-right), HD 163607 (bottom-left), HD 168443 (bottom-right). The orbits of the system planets are shown as solid lines and the Solar System planets are included as dashed lines for comparison.

For exoplanetary systems in which there is significant orbital eccentricity present, one must take care to prevent mis-interpretation of the radial velocity data. There are several ambiguities which can arise including confusing an eccentric orbit with 2:1 resonant systems (Anglada-Escudé et al. 2010), 1:1 resonant co-orbital planets (“Trojan pairs”) (Laughlin & Chambers 2002; Giuppone et al. 2012), and circular planets with long-period companions (Rodigas & Hinz 2009). A concise summary of these confusion issues is described by Wittenmyer et al. (2013) in which they test single planet eccentric systems for multiplicity.

The analysis we present here focuses on four systems: HD 37605, HD 74156, HD 163607, and HD 168443. A top-down view of each of these systems is shown in Figure 1 in which the orbits of both system planets are shown (solid lines) along with orbits of the Solar System planets for scale purposes (dashed lines). The criteria for select-

ing these systems was twofold. Firstly, the system was required to be a multi-planet system in which the inner planet has an eccentricity greater than 0.5. Secondly, the system must have sufficient data, including at least one complete orbital phase of the outer planet, to minimize the potential confusion issues mentioned above.

HD 37605b was the first planet discovered using the Hobby-Eberly Telescope (Cochran et al. 2011). Further studies by Wang et al. (2012) refined the orbit of the inner planet as well as detecting an additional planet in a long-period orbit. The HD 74156 system was discovered by Naef et al. (2004) using ELODIE data. The orbits of the both planets were further refined by (Meschiari et al. 2011) using Keck/HIRES data. The HD 163607 system was another case in which both planets were announced simultaneously, this time by Giguere et al. (2012) with Keck/HIRES data. HD 168443b was discovered by Marcy et al. (1999), who also detected evidence of a

TABLE 1
SYSTEM PARAMETERS

Parameter	HD 37605 ⁽¹⁾		HD 74156 ⁽²⁾	
	b	c	b	c
M_* (M_\odot)	1.000 ± 0.050		1.24	
P (days)	55.01307 ± 0.00064	2720 ± 57	51.638 ± 0.004	2520 ± 15
T_p ⁽⁵⁾	13378.241 ± 0.020	14838 ± 581	10793.3 ± 0.2	8416 ± 33
e	0.6767 ± 0.0019	0.013 ± 0.015	0.63 ± 0.01	0.38 ± 0.02
ω (deg)	220.86 ± 0.28	221 ± 78	174 ± 2	268 ± 4
K (m s^{-1})	202.99 ± 0.72	48.90 ± 0.86	108 ± 4	115 ± 3
$M_p \sin i$ (M_J)	2.802 ± 0.011	3.366 ± 0.072	1.78 ± 0.04	8.2 ± 0.2
a (AU)	0.2831 ± 0.0016	3.814 ± 0.058	0.29169 ± 0.00001	3.90 ± 0.02

Parameter	HD 163607 ⁽³⁾		HD 168443 ⁽⁴⁾	
	b	c	b	c
M_* (M_\odot)	1.09 ± 0.02		0.995 ± 0.019	
P (days)	75.29 ± 0.02	1314 ± 8	58.11247 ± 0.0003	1749.83 ± 0.57
T_p ⁽⁵⁾	14185.00 ± 0.24	15085 ± 880	15626.199 ± 0.024	15521.3 ± 2.2
e	0.73 ± 0.02	0.12 ± 0.06	0.52883 ± 0.00103	0.2113 ± 0.00171
ω (deg)	78.7 ± 2.0	265 ± 93	172.923 ± 0.139	64.87 ± 0.5113
K (m s^{-1})	51.1 ± 1.4	40.4 ± 1.3	475.133 ± 0.9102	297.70 ± 0.618
$M_p \sin i$ (M_J)	0.77 ± 0.04	2.29 ± 0.16	7.659 ± 0.0975	17.193 ± 0.21
a (AU)	0.36 ± 0.01	2.42 ± 0.01	0.2931 ± 0.00181	2.8373 ± 0.018

⁽¹⁾ Wang et al. (2012)

⁽²⁾ Meschiari et al. (2011)

⁽³⁾ Giguere et al. (2012)

⁽⁴⁾ Pilyavsky et al. (2011)

⁽⁵⁾ JD - 2,440,000

trend due to an additional planet. This trend was later confirmed to be a second planet by Marcy et al. (2001). The orbits of both planets were later refined by Pilyavsky et al. (2011).

We summarize the Keplerian orbital solutions for each of these systems in Table 1. These are the parameters used throughout the remainder of the paper to perform analyses of the orbits. One striking feature seen in Figure 1 and Table 1 is that these particular kinds of systems are all approximately the same size scale. This is not a selection effect nor due to observational bias since the detection of the outer planet resulted from continued monitoring. The semi-major axes of the planets range between 0.28–0.36 AU and 2.4–3.9 AU for the inner and outer planets respectively. To quantify the similarity of the system size scales, we compared these systems with others by extracting orbital data for all 2-planet systems detected using the radial velocity method from the Exoplanet Data Explorer⁴ (Wright et al. 2011). The data are current as of 27th September 2013. Figure 2 plots the semi-major axes of the inner planet as a function of the ratio of outer to inner planet semi-major axes. For the four systems considered here, these ratios are 13.47, 13.37, 6.72, 9.68 for HD 37605, HD 74156, HD 163607, and HD 168443 respectively (depicted as stars in Figure 2). Note that HD 37605 and HD 74156 are almost identical in this respect and so are almost indistinguishable in Figure 2. All four systems occupy a relatively small fraction of the known distribution shown in this figure, possibly due to the dynamical constraints imposed by the eccentricity of the inner planet.

3. LIMITS ON ADDITIONAL PLANETS

Before we investigated the dynamical interactions of the 2-planet systems, we first tested both the Keple-

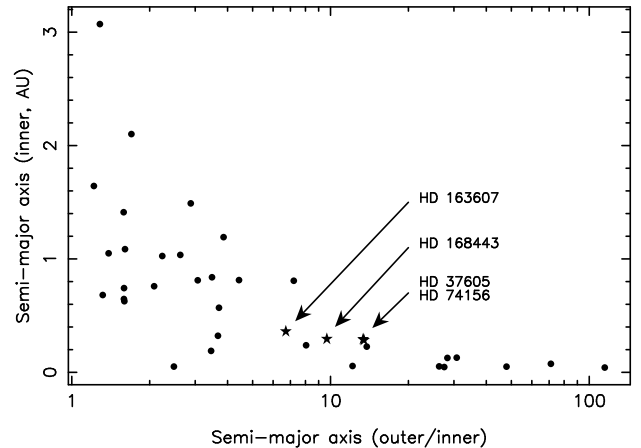


FIG. 2.— This plot includes all 2-planet systems detected using the radial velocity technique. The semi-major axis of the inner planet is plotted as a function of the ratio of the outer to inner planet semi-major axes. The locations of the four systems studied in this paper are shown as stars.

rian orbital solutions previously found (see Table 1) and determined if the residuals may disguise the presence of further planetary companions. The radial velocity data were obtained from the published literature and from the NASA Exoplanet Archive⁵ (Akeson et al. 2013). We fit the radial velocity data using the partially linearized, least-squares fitting procedure described in Wright & Howard (2009) and estimated parameter uncertainties using the BOOTTRAN bootstrapping routines described in Wang et al. (2012). We obtained Keplerian orbital solutions consistent with those described in Table 1 and thus adopt the rms residuals of those analyses.

The rms residuals are used to place 1–3 σ thresholds

⁴ <http://exoplanets.org/>

⁵ <http://exoplanetarchive.ipac.caltech.edu/>

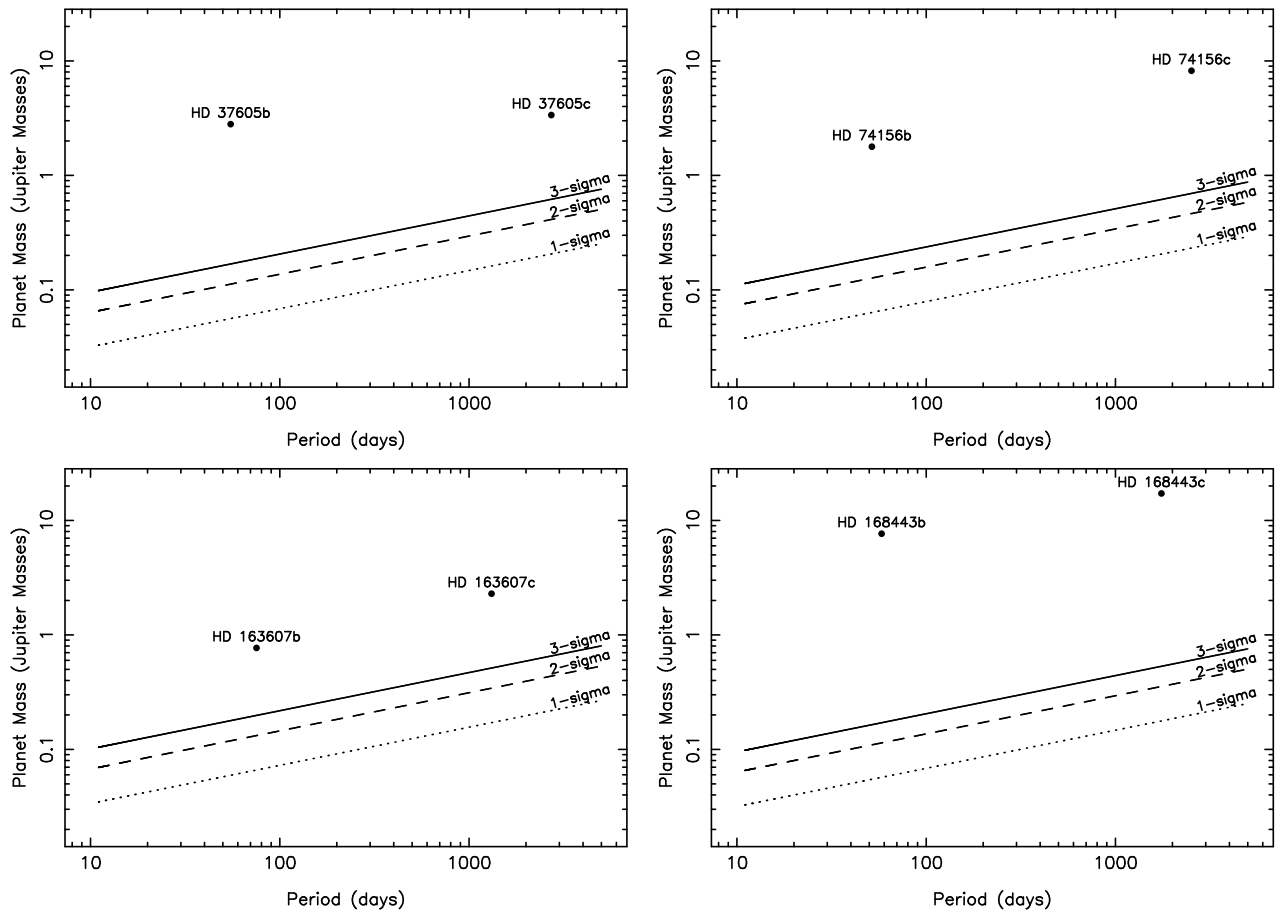


FIG. 3.— Exclusion regions (above the lines) for additional planets with the HD 37605 (top-left), HD 74156 (top-right), HD 163607 (bottom-left), and HD 168443 (bottom-right) systems. The 1–3 σ exclusion boundaries are based upon the rms scatter of the residuals to radial velocity data after the best-fit Keplerian model has been removed. The detected planets in each system are shown for reference.

which limits the presence of additional planetary companions in each system as a function of both planetary mass and orbital period. This is achieved using the maximum semi-amplitude of the radial velocity allowed by the residuals. This is expressed as

$$K = \left(\frac{2\pi G}{P} \right)^{1/3} \frac{M_p \sin i}{(M_\star + M_p)^{2/3} \sqrt{1 - e^2}} \quad (1)$$

where P is the period, i is the inclination of the planetary orbit, e is the eccentricity, and M_p and M_\star are the masses of the planet and parent star respectively. We assume a circular orbits which is a reasonable assumption for all but high eccentricities which would likely render the system unstable. The resulting mass limit thresholds are shown for each system in Figure 3. In each case the 3σ threshold lies substantially below the mass range of the two known planets. Due to the similarity in both the amplitude of the residuals and the mass of the system host stars, the constraints on possible undetected planetary masses as a function of orbital period is almost identical for all four systems. The similarity of the systems is further emphasized by the use of identical axis scales on each of the plots.

For each system, there is usually a combination of radial velocity data sources which often result in the rms scatter of the fit residuals being dominated by one or

TABLE 2
PLANETARY UPPER MASS LIMITS

System	3 σ mass limit (M_J)	
	$P = 100$ days	$P = 1000$ days
HD 37605	0.20	0.44
HD 74156	0.24	0.51
HD 163607	0.22	0.47
HD 168443	0.20	0.44

more of those sources. In these situations we adopt the rms scatter for the highest quality data to establish the limits of additional planets described here. For HD 37605, the rms scatter of the residuals is 7.61 m s^{-1} when HET data are included but the Keck/HIRES data alone produce residuals of 2.08 m s^{-1} . For HD 74156, the rms scatter of 12.8 m s^{-1} is dominated by CORALIE and ELODIE data. The rms scatter of the Keck data residuals alone is 3.5 m s^{-1} . The radial velocity data for both HD 163607 and HD 168443 were obtained exclusively from Keck/HIRES and the resulting rms scatter of the residuals is 2.9 m s^{-1} and 3.9 m s^{-1} respectively.

The planetary upper limits imposed by this analysis for each system are shown in Table 2 at orbital periods of 100 and 1000 days. This shows similar results of planets more massive than $0.2\text{--}0.5 M_J$ being excluded from lying between the known planets at the 3σ level. This

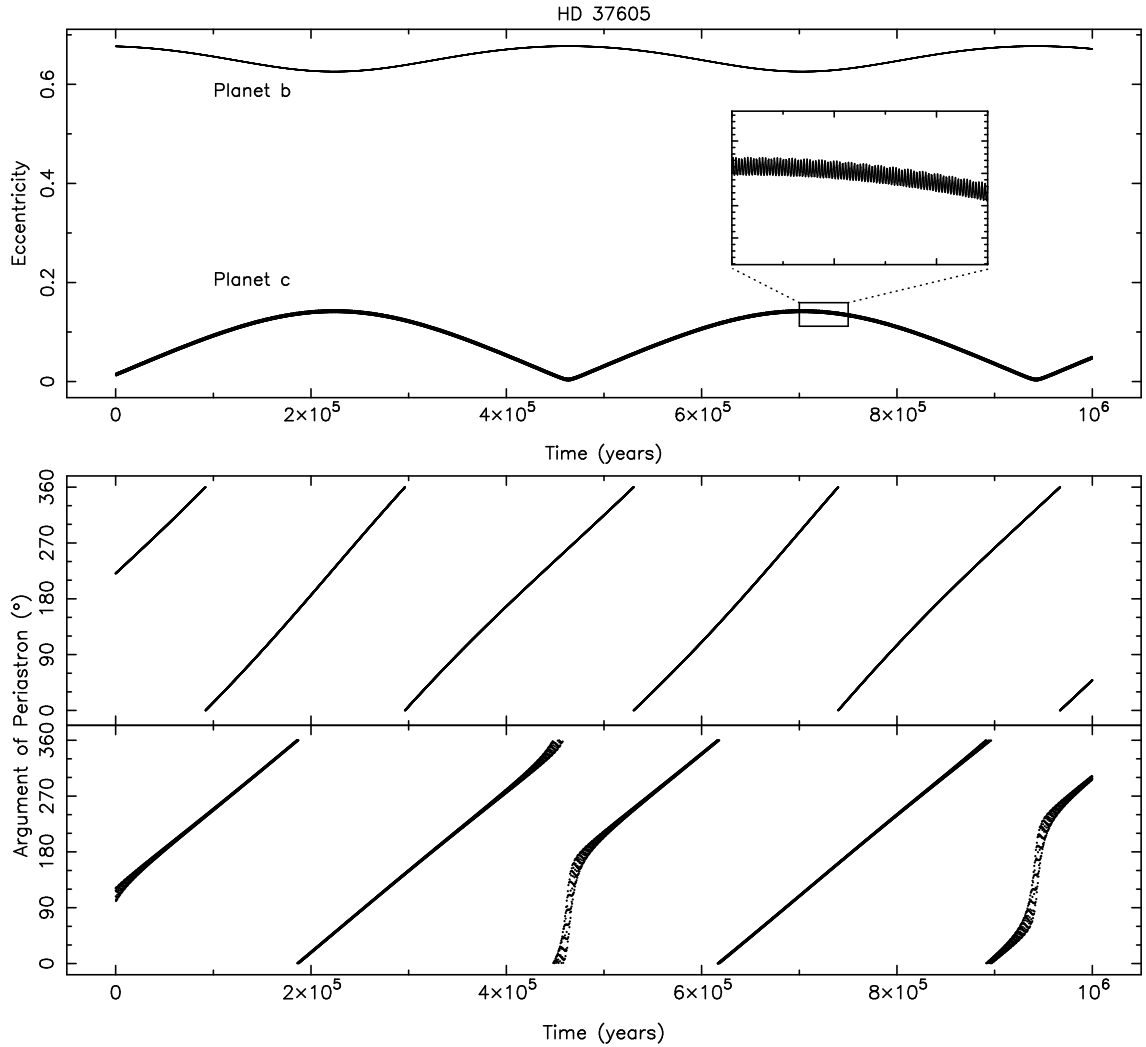


FIG. 4.— Dynamical simulations of the HD 37605 system, showing the eccentricity oscillations of both planets (top panel) and the periastron precession of the b planet (middle panel) and c planet (bottom panel). The zoom window in the top panel shows a simulation period of 50,000 years.

is likely due to instability regions imposed by the oscillating eccentricities of the much more massive inner and outer planet. We explore these oscillations in the following section.

4. DYNAMICAL ANALYSIS

The stability of exoplanetary systems has been explored in considerable depth by such authors as Chambers et al. (1996); Barnes & Greenberg (2006b, 2007). In this section we examine the dynamical interactions of the four particular two-planet systems which are the subject of this paper. The N-body integrations required for the dynamical simulations were performed by utilizing the Mercury Integrator Package, described in more detail by Chambers (1999). For these simulations, we adopted the hybrid symplectic/Bulirsch-Stoer integrator. We also used a Jacobi coordinate system which generally provides more accurate results for multi-planet systems (Wisdom & Holman 1991; Wisdom 2006) except in cases of close encounters (Chambers 1999). The integrations were performed for a simulation of 10^6 years, in steps of 100 years, starting at the present epoch.

4.1. The HD 37605 System

The initial eccentricity and argument of periastron for the HD 37605 b and c planets are 0.6767, 220° and 0.013, 221° respectively (see Table 1). The results of the N-body integrations are plotted in Figure 4. The eccentricity oscillations shown in the top panel complete approximately two cycles during the 10^6 year simulation. The range of eccentricity for the b and c planets are 0.626–0.677 and 0.001–0.145 respectively. Thus, in this case, the amplitude of the eccentricity variations for the outer planet exceeds that of the inner planet.

These results have several details of note. Firstly, the high-amplitude eccentricity oscillations of the outer planet are comprised of smaller-amplitude higher-frequency oscillations. This is shown by the zoomed-in region in the top panel of Figure 4 which has a time-span of 50,000 years. The amplitude of these higher-frequency oscillations is ~ 0.05 with a period of ~ 550 years. Secondly, the periastron arguments of the planets begin closely aligned (see Table 1) but differing precession rates result in them being slightly out of sync with each other. The precession of the inner planet

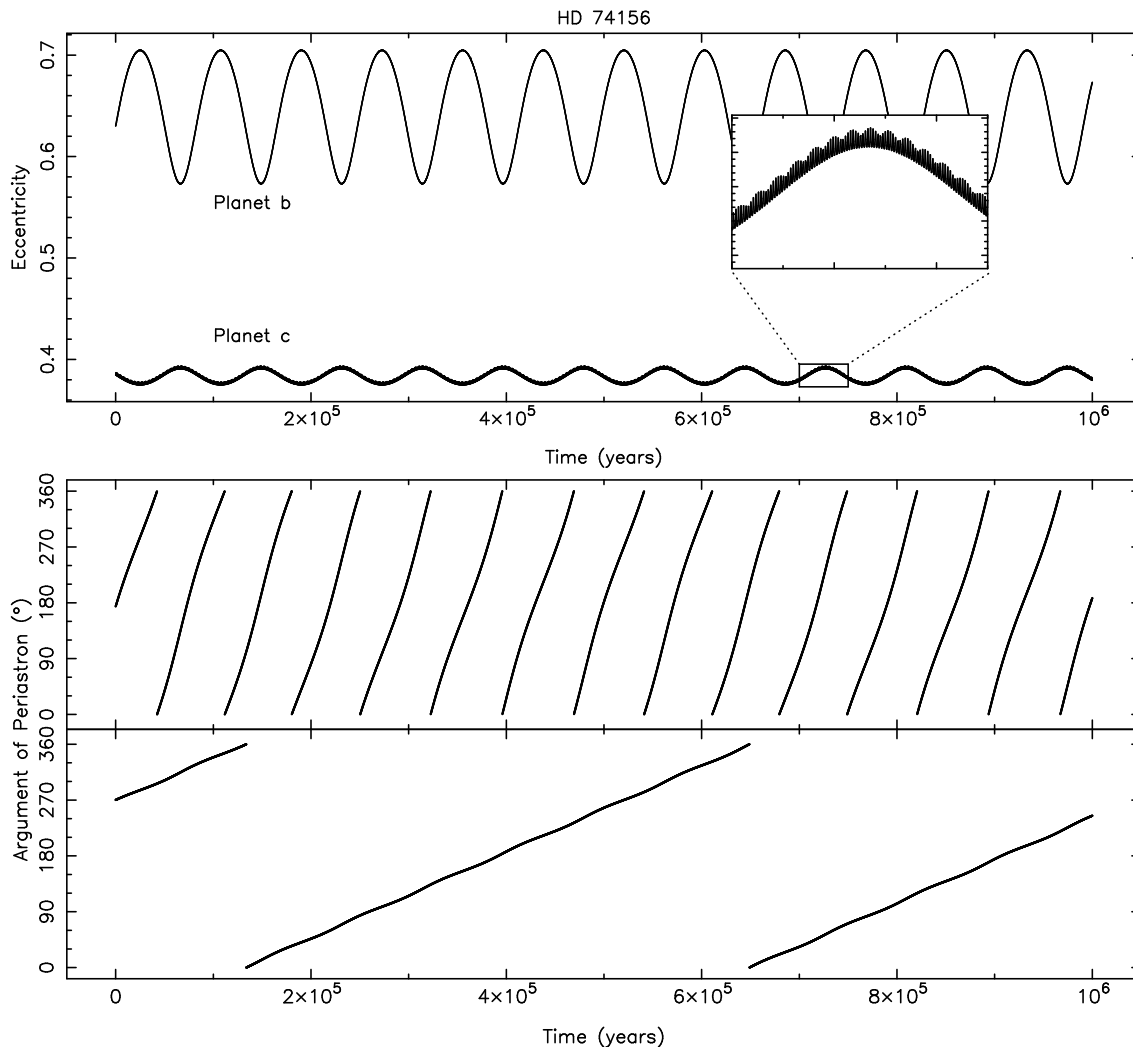


FIG. 5.— Dynamical simulations of the HD 74156 system, showing the eccentricity oscillations of both planets (top panel) and the periastron precession of the b planet (middle panel) and c planet (bottom panel). The zoom window in the top panel shows a simulation period of 50,000 years.

($0.164^\circ/\text{century}$) is slightly higher than that for the outer planet ($0.14^\circ/\text{century}$). Note also that during those moments when the eccentricity of the outer planet is ~ 0.0 then the periastron argument becomes highly uncertain (since ω is undefined when $e = 0.0$) resulting in a dispersion of the ω values near those times. For this reason the evolution of the periastron argument for the outer planet is difficult to determine and may possibly match that of the inner planet.

4.2. The HD 74156 System

The HD 74156 system differs from the other three in this study in that both the mass ratio of the two planets and the eccentricity of the outer planet are the highest of all four systems. As shown in Figure 1 and Table 1, the orientation of the orbits are not closely aligned as was the case for HD 37605. The N-body integration results for HD 74156 are plotted in Figure 5. The eccentricity oscillations for both planets shown in the top panel complete approximately 12 cycles during the 10^6 year simulation. The range of eccentricity for the b and c planets are 0.573–0.705 and 0.375–0.394 respectively. The ma-

ior eccentricity variation in this case occurs for the inner planet whereas the variations for the outer planet are far more subtle. The high-frequency oscillations shown in the zoom-in window of the top panel of Figure 5 show evidence of vibrational beating with an amplitude that is negligible compared with the low-frequency oscillations. Although the first-order eccentricity oscillations of the planets share the same frequency, the periastron precessions (shown in the bottom two panels) do not. The precession rates of the inner and outer planet are $0.05^\circ/\text{century}$ and $0.007^\circ/\text{century}$ respectively.

4.3. The HD 163607 System

Of the four systems, the HD 163607 system contains both the largest orbital period and the highest eccentricity for the inner planet. Additionally, the periastron arguments for the inner and outer planets are almost perfectly anti-aligned (π out of phase) with one another. The N-body integration results for HD 163607 are plotted in Figure 6. This figure shows that both the oscillation of the eccentricities and periastron precession of the orbits ($0.06^\circ/\text{century}$) remain approximately in sync for

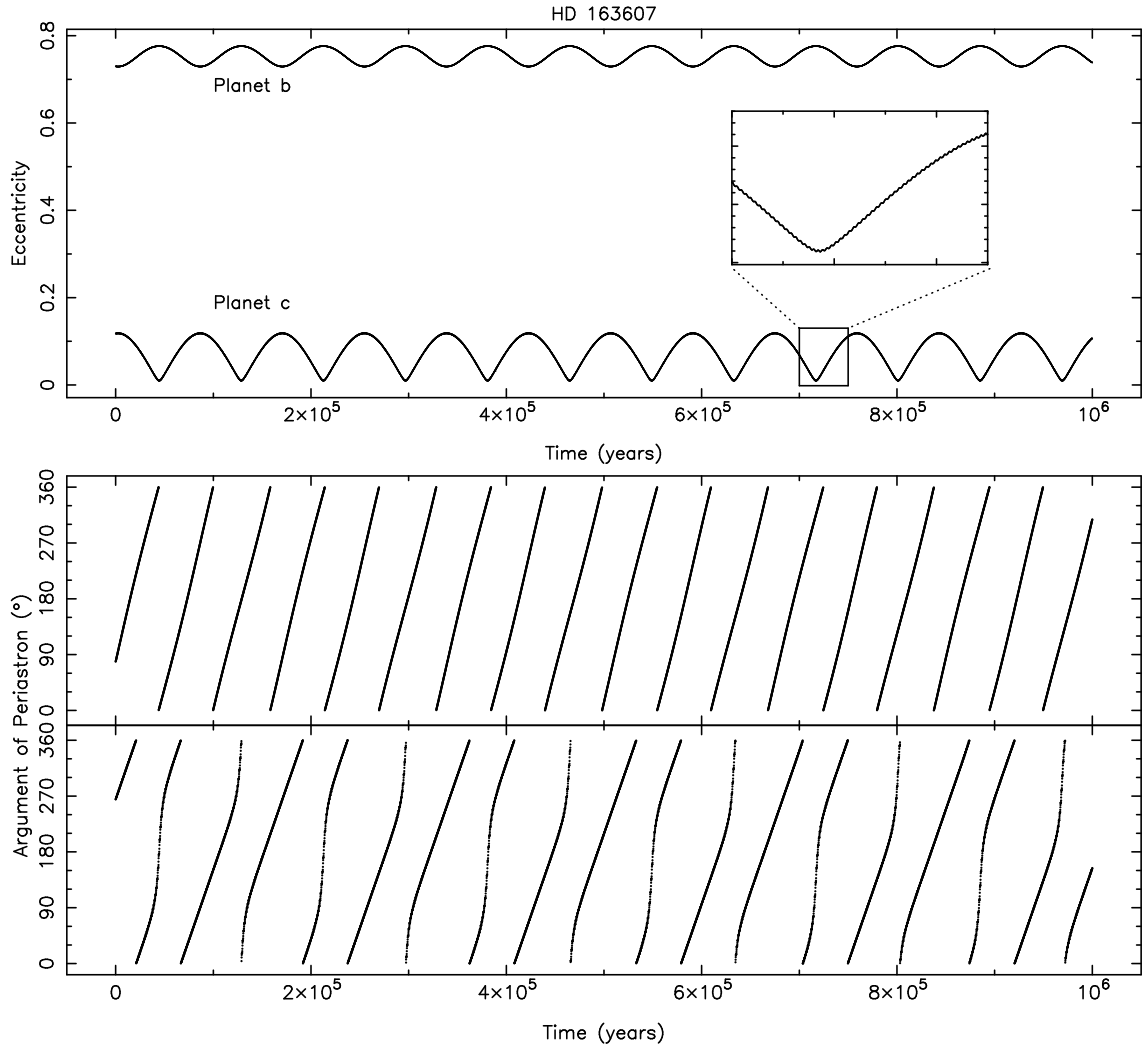


FIG. 6.— Dynamical simulations of the HD 163607 system, showing the eccentricity oscillations of both planets (top panel) and the periastron precession of the b planet (middle panel) and c planet (bottom panel). The zoom window in the top panel shows a simulation period of 50,000 years.

the two planets during the 100,000 year simulation. Note also that the outer planet also exhibits higher-frequency eccentricity oscillations although at a much smaller amplitude than for the outer planet in the other three systems (see the zoom-in window in the top panel of Figure 6). The range of eccentricity for the b and c planets are 0.729–0.776 and 0.009–0.119 respectively. Thus, the major oscillations occur for the outer planet. The eccentricity of the outer planet is periodically forced to zero which produces a similar ambiguity in the periastron argument as was seen in the case of HD 37605 (see Section 4.1).

4.4. The HD 168443 System

The stability of the HD 168443 system has been previously studied by Barnes & Quinn (2004) in which they found that the system is stable although weak interactions occur between the two planets. The revised orbital parameters provided by Pilyavsky et al. (2011) do not result in a substantial change to the conclusion of system stability. The planets of the HD 168443 system have the largest minimum masses of all four systems. This results in substantially increased interactions be-

tween the two planets and a relatively high-frequency of both the eccentricity oscillations and periastron precession of the orbits. The results of the N-body integration for HD 168443 are shown in Figure 7. The range of eccentricity for the b and c planets are 0.500–0.607 and 0.210–0.265 respectively. Although the eccentricity oscillations have almost the same frequency, the amplitude of the outer planet oscillations are almost half that of the inner planet and have a high-frequency component as seen in the other three systems. The periastron precession rate of the inner planet is substantial: $0.23^\circ/\text{century}$ compared with $0.06^\circ/\text{century}$ for the outer planet.

5. MUTUAL INCLINATIONS

Here we briefly investigate the effect of introducing a mutual inclination into the results of our simulations and the predicted angular momentum exchange. We performed this investigation for the HD 163607 system since the results for this system shown in Section 4 yield the most well-defined eccentricity oscillations of the four systems considered. To do this, we repeated the N-body integrations with mutual orbital inclinations from 0° to 90° in increments of 5° . Shown in Figure 8 are the results

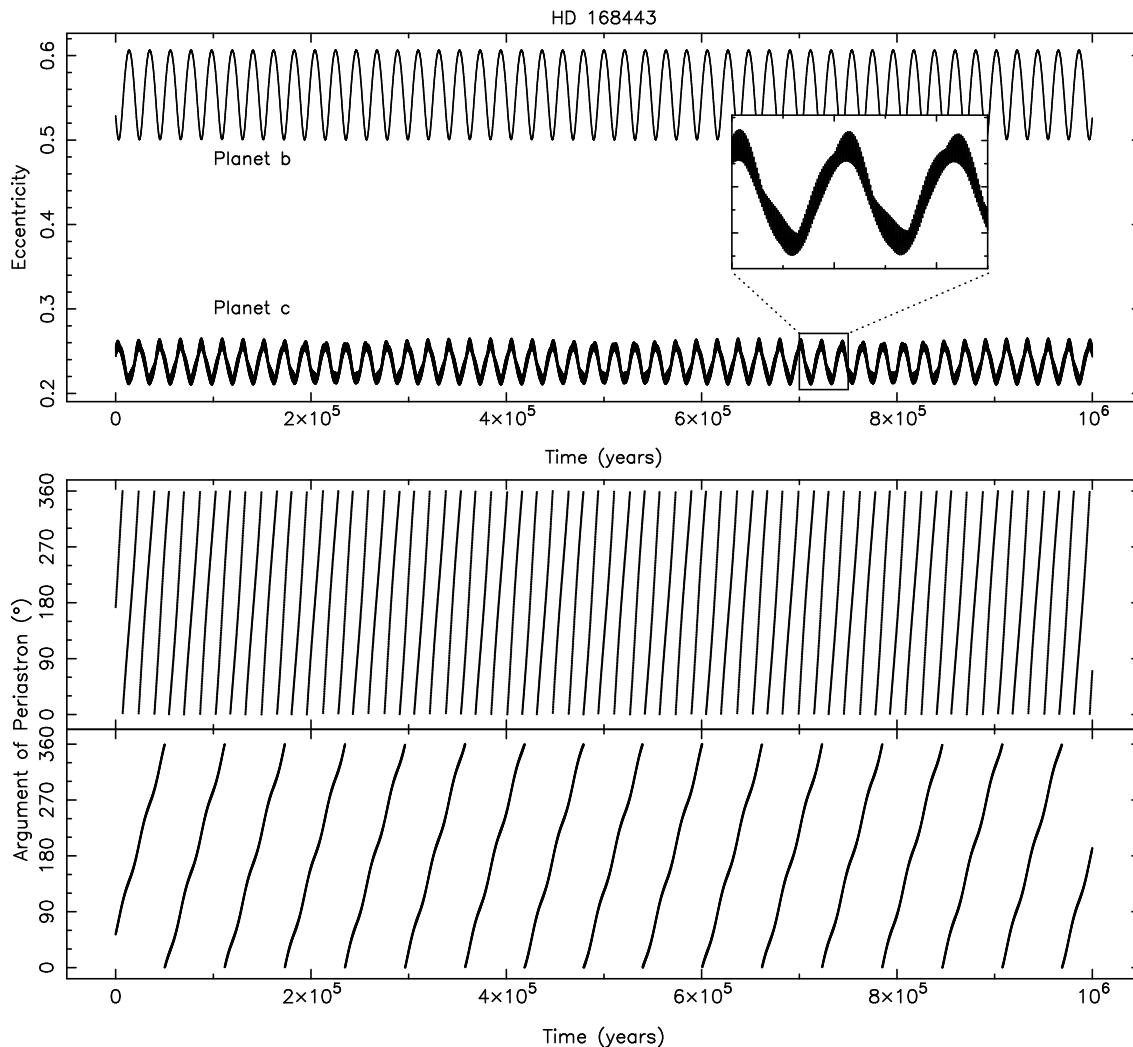


FIG. 7.— Dynamical simulations of the HD 168443 system, showing the eccentricity oscillations of both planets (top panel) and the periastron precession of the b planet (middle panel) and c planet (bottom panel). The zoom window in the top panel shows a simulation period of 50,000 years.

for 5° and 10° mutual inclinations where the eccentricity evolution of the b planet is shown for the full 100,000 year simulation.

The effect of introducing a mutual inclination is to increase the amplitude of both the primary (low-frequency) and secondary (high-frequency) oscillations. This increase in oscillation amplitude increases with increasing mutual inclination until the inner planet is ejected from the system, the timescale of which depends on the amount of mutual inclination present. For example, the HD 163607 system does not remain stable for the full 100,000 year simulation for mutual inclinations larger than 60° . Although the amplitude of the secondary oscillations increases with increasing mutual inclination (see Figure 8), the frequency of the oscillations remains the same. Thus it would require several hundred years of observations (in the case of HD 163607) in order to detect the extent of the mutual inclination from such eccentricity variations.

6. ORIGIN OF SYSTEMS WITH UNEQUAL ECCENTRICITIES

We have attempted to understand the origin of these systems with large differences in eccentricity. The large eccentricities of exoplanets are thought to be the scars of past planet-planet scattering events (Adams & Laughlin 2003; Chatterjee et al. 2008; Jurić & Tremaine 2008). We mined a dataset of simulations of planet-planet scattering to determine what conditions were required to create such systems.

The simulations we used were presented in several previous studies of planet-planet scattering and its consequences (Raymond et al. 2008, 2009, 2010; Timpe et al. 2013). We focused on a particular set of simulations referred to as the mixed set in previous papers. These simulations started from three giant planets with masses between one Saturn mass and $1000M_\oplus$ (roughly 3 Jupiter masses), chosen to follow a $dN/dM \propto M^{-1.1}$ distribution (Butler et al. 2006). The planets were initially placed on circular orbits with small mutual inclinations between a few and ten AU, spaced by 4-5 mutual Hill radii. About 60% of the simulations became unstable within 100 Myr.

Our sample consists of 448 simulations in which two planets survived (and energy was adequately conserved).

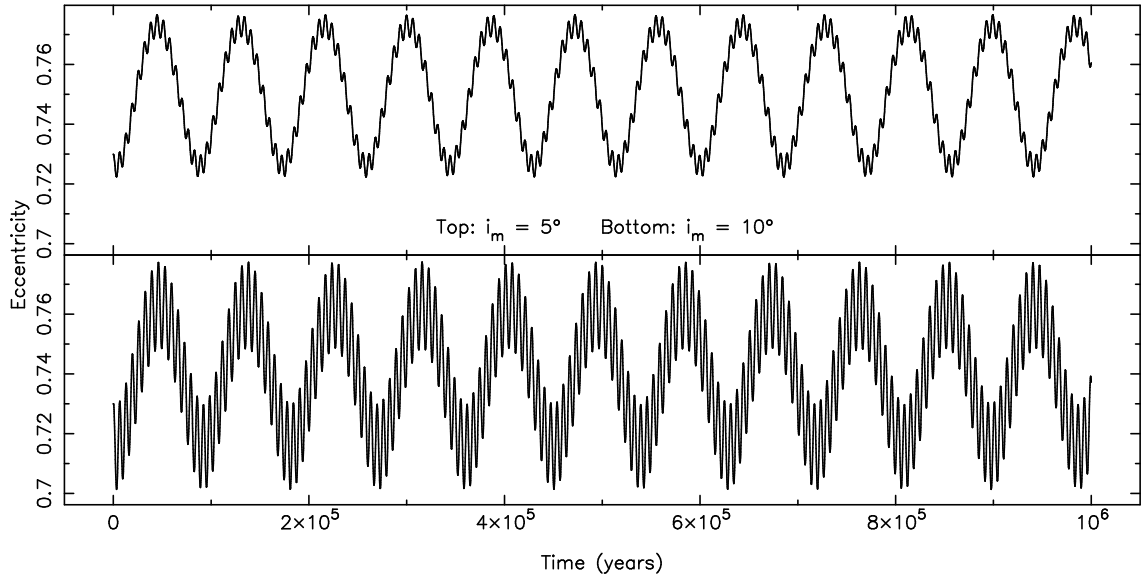


FIG. 8.— The effect of introducing mutual inclination (i_m) to the HD 163607 system on the eccentricity evolution of planet b. Top panel: $i_m = 5^\circ$. Bottom panel: $i_m = 10^\circ$.

14 systems (3.1% of the sample) contained an outer planet on an eccentric orbit ($e_{outer} > 0.5$) and a significantly less-eccentric inner planet ($e_{inner} < 0.25$). These represent potential analogs to the systems studied in this paper.

The 14 potential analogs differed from the rest of the sample in two ways. First, the innermost planet – both at the start and end of the simulations – was systematically more massive than the outer planet(s). A K-S test showed that the difference between the potential analogs and the other simulations was statistically significant, with $p = 3 \times 10^{-3}$. The number of encounters undergone during the scattering process was higher for the potential analogs but with a lower statistical significance ($p = 0.03$). In essence, the analog systems were created by multiple scattering between planets in the outer parts of their systems and this scattering was only weakly coupled to the more massive, inner planet.

The mass ratios between the surviving planets are again different between the control sample and the potential analogs. The potential analogs have a higher inner-to-outer planetary mass ratio with a strong statistical significance ($p = 7 \times 10^{-4}$). This is because a more massive inner planet is less affected by the scattering between outer planets and thus keeps a smaller eccentricity. However, the four systems that we study here all have more massive outer planets.

There was only one analog system with a more massive outer planet. In that system the planetary instability was system-wide. The inner planet was initially scattered outward by the middle planet, then back inward by the outer planet. The planet that was initially the middle one was then scattered outward, was again repeatedly scattered by the roughly equal-mass outer planet and eventually ejected from the system. The outer planet’s large eccentricity was a result of its having been scattered off a similar-sized planet, scattering among equal-mass planets representing the strongest possible eccentricity increase (Raymond et al. 2010).

To explain the observed systems we therefore need to

invoke strong scattering events with specific characteristics. The scattering must have most strongly affected the outermost observed planet and it must have included a roughly equal-mass planet that was ejected. The innermost, less massive planet, must have been sufficiently removed from this scattering to survive on a lower eccentricity orbit (clearly seen in Figure 2 by the large orbital separations in these systems). The most likely origin of such conditions would therefore be systems in which two or more high-mass planets formed on wider orbits than an inner, lower-mass planet.

Of course, this assumes a self-unstable system. There is also the possibility of an outside-in perturbation on the system from a passing star or wide binary (Zakamska & Tremaine 2004; Malmberg et al. 2007; Kaib et al. 2013). In that case, a significant separation between the inner and outer planets is still needed to avoid transmitting the perturbation all the way to the inner parts of the system.

7. DISCUSSION

An aspect of interest in the orbital configurations of the systems studied here is the origin and subsequent evolution of those orbits (see Section 6). Veras & Ford (2009) showed that finding these kinds of systems at a particular epoch can have a low associated probability. For example, Figure 4 reveals that the c planet in the HD 37605 system spends the majority of its orbit at a significantly higher eccentricity than that which is currently observed. It is also unlikely that the planets would have formed in such orbits without significant transfers of angular momentum to an additional component (stellar or planetary) no longer present in the system. Thus, an important property of these systems with eccentricity diversity is the angular momentum deficit (AMD), which is the difference in angular momentum of the system compared with the angular momentum if the planets were in circular orbits with the same semi-major axes. This is

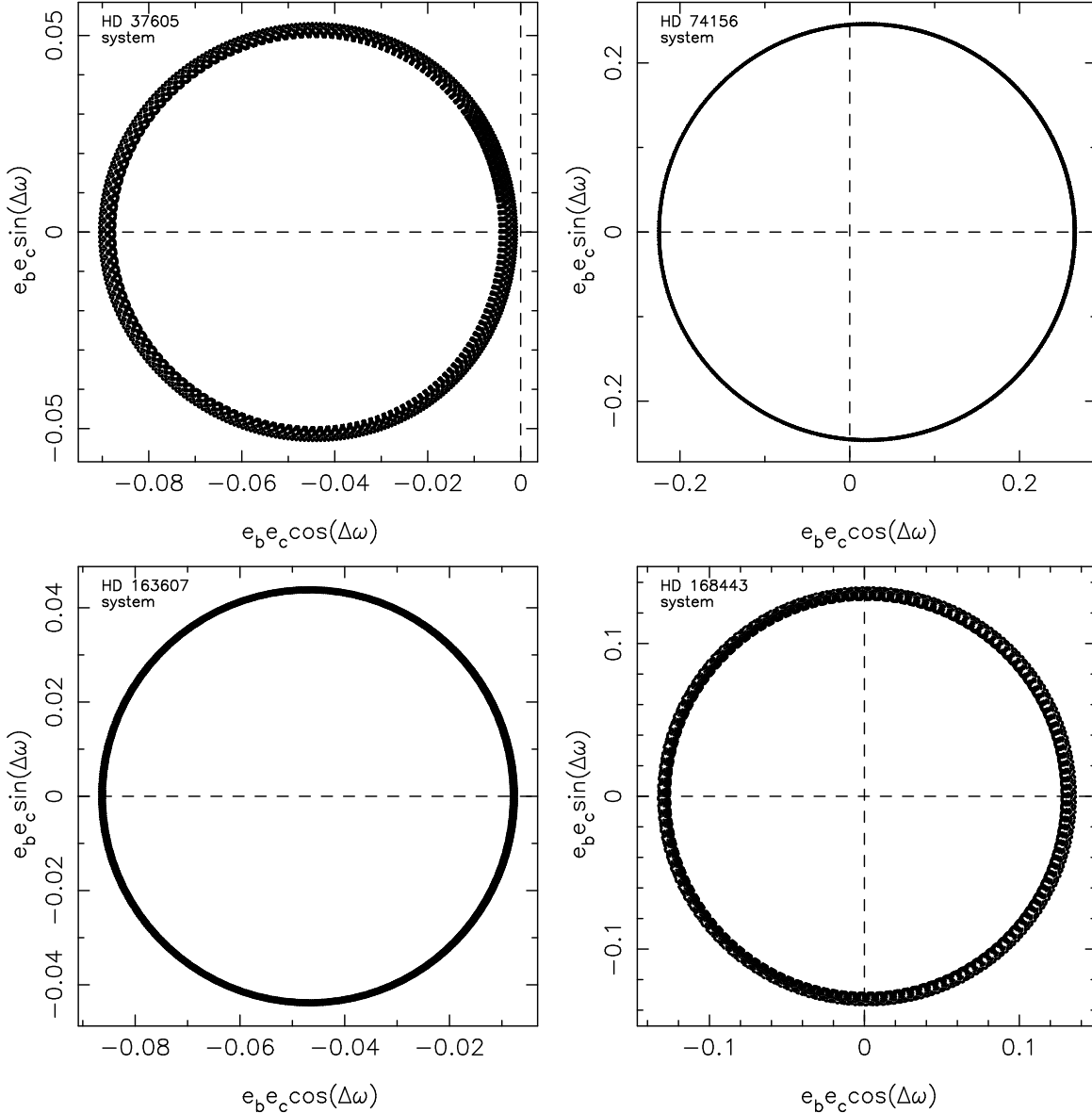


FIG. 9.— A polar plot of $e_b e_c$ versus $\Delta\omega$ for each of the four systems described in this paper: HD 37605 (top-left), HD 74156 (top-right), HD 163607 (bottom-left), HD 168443 (bottom-right). According to the criteria of Barnes & Greenberg (2006c), the apsidal modes are librating for HD 37605 and HD 163607, and circulating for HD 74156 and HD 168443.

given by the following equation:

$$\text{AMD} \equiv \sum_{i=1}^N L_p \left(1 - \sqrt{1 - e_i^2} \right) \quad (2)$$

where

$$L_p = \frac{M_{p,i} M_\star}{M_{p,i} + M_\star} \sqrt{G(M_{p,i} + M_\star) a_i} \quad (3)$$

is the angular momentum of a circular orbit for planet i . In cases where $M_{p,1} \sim M_{p,2}$, such as HD 37605, the inner planet has much less orbital angular momentum than the outer planet resulting in larger eccentricity oscillations for a given AMD value.

The system with the smallest eccentricity oscillations is HD 74156. As noted in Section 4.2, this is also the system with the highest planetary mass ratio and eccentricity of

the outer planet. These facts combined with the relatively slow periastron precession of the outer planet are consistent with the findings of Barnes & Quinn (2004) that the system is unlikely to possess unstable configurations. Calculations of the AMD for these systems show that the HD 74156 system has a substantially higher (factor of 2) AMD than the other three.

The various types of apsidal motion in interacting exoplanetary systems have been investigated in detail by Barnes & Greenberg (2006a,c). Barnes & Greenberg (2006c) distinguish between two basic types of apsidal behavior, libration and circulation, where the boundary between them is referred to as a secular separatrix. This distinction may be used as an additional tool in characterizing the long-term behavior of Keplerian orbital elements of multi-planet systems. Figure 9 represents the apsidal trajectory graphically for the four systems dis-

cussed here. The plot uses the eccentricity of the inner and outer planets (e_b and e_c respectively) and the difference in periastron arguments ($\Delta\omega$) to create a polar representation of the apsidal behavior. This shows that the apsidal modes of HD 74156 and HD 168443 are circulating since the polar trajectories encompass the origin. This is consistent with the relatively small amplitude of the c planet eccentricity evolutions shown in Figures 5 and 7. Conversely, HD 37605 and HD 163607 are shown to be librating systems and are close to the separatrix between secular libration and circulation. This is also consistent with Figures 4 and 6 since those show that the c planet eccentricities regularly approach zero.

Finally, it is worth considering as to whether the oscillations described here in both the eccentricity and periastron precession may be detectable in reasonable timescales. The high-frequency secondary oscillations in the eccentricity of the outer planet, such as HD 37605 and HD 168443, are of relatively low amplitude. The orbital precession of exoplanets has been previously investigated by Kane et al. (2012b) who found that the timescales for such precession is unlikely to allow detection except for the very short-period planets. By comparison, the perihelion precessions of Mercury and Earth are $0.159^\circ/\text{century}$ and $0.321^\circ/\text{century}$ respectively (Clemence 1947). For the cases presented in Section 4, the period of eccentricity oscillation and periastron precession are at least several centuries in even the most optimistic cases. The main hindrance however is that the uncertainties associated with those parameters tend to be comparable to the expected variations.

8. CONCLUSIONS

Exoplanet discoveries are leading to a diverse range of multi-planet system configurations. Here we have concentrated on a particular configuration which consists of two planets in which the inner planet has an eccentricity larger than 0.5. As shown in Section 2, these sys-

tems bear many similarities, in particular the ratio of the outer to inner planet semi-major axes which is likely a constraint imposed by the unique dynamics present in these systems. Through an examination of the residuals to the radial velocity fits to the data, we are able to exclude the presence of planets with masses larger than $\sim 0.5M_J$ with orbital periods less than 1000 days at the 3σ level.

Our N-body integrations of each system show that there is a synchronous transfer of angular momentum between the planets in most cases. The case of HD 74156 is interesting due to the high mass ratio, the relatively small amplitude of eccentricity oscillation and periastron precession of the outer planet, and the relatively high AMD for the system. The high-frequency secondary eccentricity oscillations for the outer planets is indicative of outer planet responses to frequent dynamical interactions with the much shorter period inner planet. The effect of introducing a mutual inclination is to increase the amplitude of secondary oscillations in the inner planet until that planet is subsequently ejected from the system. The AMDs of these systems provide indications that these systems have indeed had a significant perturbation event which produced these relatively rare orbital configurations. As more of these kinds of systems are discovered, we can gain further understanding as to their frequency and dynamical histories.

ACKNOWLEDGEMENTS

The authors would like to thank the anonymous referee, whose comments greatly improved the quality of the paper. This research has made use of the Exoplanet Orbit Database and the Exoplanet Data Explorer at exoplanets.org. This research has also made use of the NASA Exoplanet Archive, which is operated by the California Institute of Technology, under contract with the National Aeronautics and Space Administration under the Exoplanet Exploration Program.

REFERENCES

- Adams, F.C., Laughlin, G. 2003, *Icarus*, 163, 290
Akeson, R.L., et al. 2013, *PASP*, 125, 989
Anglada-Escudé, G., López-Morales, M., Chambers, J.E., 2010, *ApJ*, 709, 168
Barnes, R., Quinn, T. 2004, *ApJ*, 611, 494
Barnes, R., Greenberg, R. 2006, *ApJ*, 638, 478
Barnes, R., Greenberg, R. 2006, *ApJ*, 647, L163
Barnes, R., Greenberg, R. 2006, *ApJ*, 652, L53
Barnes, R., Greenberg, R. 2007, *ApJ*, 665, L67
Butler, R.P., et al., 2006, *ApJ*, 646, 505
Chambers, J.E., Wetherill, G.W., Boss, A.P. 1996, *Icarus*, 119, 261
Chambers, J.E. 1999, *MNRAS*, 304, 793
Chatterjee, S., Ford, E.B., Matsumura, S., Rasio, F.A. 2008, *ApJ*, 686, 580
Clemence, G.M. 1947, *RvMP*, 19, 361
Cochran, W.D., Hatzes, A.P., Butler, R.P., Marcy, G.W. 1997, *ApJ*, 483, 457
Cochran, W.D., et al. 2004, *ApJ*, 611, L133
Ford, E.B., Rasio, F.A., 2008, *ApJ*, 686, 621
Giguere, M.J., et al. 2012, *ApJ*, 744, 4
Giuppone, C.A., Benítez-Llambay, P., Beaugé, C. 2012, *MNRAS*, 421, 356
Goldreich, P., Soter, S., 1966, *Icarus*, 5, 375
Goldreich, P., Lithwick, Y., Sari, R. 2004, *ApJ*, 614, 497
Jurić, M., Tremaine, S., 2008, *ApJ*, 686, 603
Kaib, N.A., Raymond, S.N., Duncan, M. 2013, *Nature*, 493, 381
Kane, S.R., Ciardi, D.R., Gelino, D.M., von Braun, K. 2012, *MNRAS*, 425, 757
Kane, S.R., Horner, J., von Braun, K. 2012, *ApJ*, 757, 105
Laughlin, G., Chambers, J.E. 2001, *ApJ*, 551, L109
Laughlin, G., Chambers, J.E. 2002, *AJ*, 124, 592
Lin, D.N.C., Ida, S. 1997, *ApJ*, 477, 781
Malmberg, D., de Angeli, F., Davies, M.B., Church, R.P., Mackey, D., Wilkinson, M.I. 2007, *MNRAS*, 378, 1207
Malmberg, D., Davies, M.B., 2009, *MNRAS*, 394, L26
Marcy, G.W., Butler, R.P., Vogt, S.S., Fischer, D., Liu, M.C. 1999, *ApJ*, 520, 239
Marcy, G.W., et al. 2001, *ApJ*, 555, 418
Matsumura, S., Takeda, G., Rasio, F.A., 2008, *ApJ*, 686, L29
Meschiari, S., Laughlin, G., Vogt, Steven S. Butler, R.P., Rivera, E.J., Haghighipour, N., Jalowiczor, P. 2011, *ApJ*, 727, 117
Naef, D., et al. 2001, *A&A*, 375, L27
Naef, D., Mayor, M., Beuzit, J.L., Perrier, C., Queloz, D., Sivan, J.P., Udry, S. 2004, *A&A*, 414, 351
Pilyavsky, G., et al. 2011, *ApJ*, 743, 162
Rasio, F.A., Ford, E.B. 1996, *Science*, 274, 954
Raymond, S.N., Barnes, R., Armitage, P.J., Gorelick, N. 2008, *ApJ*, 687, L107
Raymond, S.N., Armitage, P.J., Gorelick, N. 2009, *ApJ*, 699, L88
Raymond, S.N., Armitage, P.J., Gorelick, N. 2010, *ApJ*, 711, 772
Rodigas, T.J., Hinz, P.M. 2009, *ApJ*, 702, 716
Timpe, M., Barnes, R., Kopparapu, R., Raymond, S.N., Greenberg, R., Gorelick, N. 2013, *AJ*, 146, 63
Veras, D., Ford, E.B. 2009, *ApJ*, 690, L1

- Wang, J., Ford, E.B., 2011, MNRAS, 418, 1822
Wang, S.X., et al. 2012, ApJ, 761, 46
Weidenschilling, S.J., Marzari, F. 1996, Nature, 384, 619
Wisdom, J., Holman, M. 1991, AJ, 102, 1528
Wisdom, J. 2006, AJ, 131, 2294
- Wittenmyer, R.A., et al. 2013, ApJS, 208, 2
Wright, J.T., Howard, A.W. 2009, ApJS, 182, 205
Wright, J.T., et al. 2011, PASP, 123, 412
Zakamska, N.L., Tremaine, S. 2004, AJ, 128, 869